MRS Communications (2015), 5, 235–242
© Materials Research Society, 2015
doi:10.1557/mrc.2015.37

MRS Communications

Polymers/Soft Matter Research Letter

Continuous and patterned deposition of functional block copolymer thin films using electrospray

Hanqiong Hu and **Kristof Toth,** Department of Chemical and Environmental Engineering, Yale University, New Haven, Connecticut 06511, USA
Myungwoong Kim, Department of Chemistry, Inha University, Incheon 402-751, Republic of Korea
Padma Gopalan, Department of Materials Science and Engineering, University of Wisconsin, Madison, Wisconsin 53706, USA
Chinedum O. Osuji, Department of Chemical and Environmental Engineering, Yale University, New Haven, Connecticut 06511, USA
Address all correspondence to Chinedum Osuji at **chinedum.osuji@yale.edu**

(Received 7 February 2015; accepted 26 May 2015)

Abstract

We report the use of electrospray to continuously deposit thin films, including patterned films, of a block copolymer (BCP). High substrate temperatures led to vertically oriented cylindrical microdomains at the film surface independent of the solvent composition and deposition rates utilized. Conversely, low substrate temperatures resulted in morphologies that were more sensitive to these parameters, with poorly ordered films of globular structures observed at the lowest temperatures considered. The deposition pattern is defined by spatially varying the electric field at the substrate using an underlying charged grid. These results open up new possibilities for patterned deposition of BCP films with morphological control.

Introduction

Block copolymers (BCPs) have been explored extensively as a platform for nanofabrication due to their self-assembly on pertinent length scales (~5–100 nm), and the versatility of available means for controlling the length scale and chemical functionality through molecular design. Properly leveraging BCP self-assembly in nanotechnology requires the ability to produce well-ordered or potentially defect-free morphologies in the relevant geometry associated with a given application. A variety of directed self-assembly methods have been developed towards these ends, as recently reviewed.[1] In thin films, manipulation of interfacial interactions is often times the salient issue for controlling morphology. In the absence of solvent, a so-called non-preferential or block neutral interface is required to produce perpendicularly oriented lamellae and cylinders by thermal annealing. This has been achieved through substrate modification using random copolymer brushes/mats[2–4] as well as self-assembled monolayers.[5,6] Solvent vapor annealing (SVA), on the other hand, utilizes film swelling and deswelling by volatilized species to accelerate ordering kinetics, manipulate interfacial interaction, and drive alignment. SVA can produce a variety of morphologies which are often kinetically trapped relative to those produced by thermal annealing under the same conditions. Recent advancements in SVA have enabled in-depth understanding of critical factors in dictating film morphology, including the selectivity of solvent, film swelling ratio, and solvent removal rate, due to more precise control of the process using flow-through setups.[7–9] Zone annealing,[10] soft shear,[11] and direct shear alignment[12] have also been successfully used to control morphology in BCP thin films.

Ordering and deposition of BCP thin films are conventionally accomplished in a sequential manner whereby material is first deposited by spin-coating or casting, followed by a period of annealing to drive development of a well-ordered morphology. A recent exciting development concerns the use of electrohydrodynamic jet printing for on-demand BCP deposition, resulting in patterns with sub-micron scale resolution, followed by thermal annealing to order the patterned material.[13] While such batch or serial processing is effective, a continuous or parallel process may provide greater utility in certain contexts, and particularly where loss of high value materials to spin-coating is not sustainable. Zone casting is an example of a processing method in which deposition and ordering take place quasi-simultaneously. It utilizes slot-die coating to slowly deposit a BCP in solution onto a moving substrate, and the evaporation of solvent from the solution to drive ordering of the BCP.[14] Another example is electrospray deposition (ESD), which provides for continuous fabrication of BCP thin films with ordered morphologies that can be thermally equilibrated or kinetically trapped, depending on the spray parameters.[15,16] The process entails delivery to a heated substrate of femtogram quantities (10^{-15} g) of material from charged sub-micron droplets of dilute solution produced by electrospray atomization. The fact that the droplets produced by electrospray atomization are charged opens up the possibility to use electric fields to spatially control BCP deposition, as has been advanced successfully for particulate systems.[17–19]

https://doi.org/10.1557/mrc.2015.37 Published online by Cambridge University Press

In this study, we report results of a systematic exploration of ESD of poly(styrene-*block*-methyl methacrylate) (PS-*b*-PMMA) thin films and examine the morphology dependence on thermal, solvent and substrate wetting effects. PS-*b*-PMMA is a widely studied functional material in which the ability to selectively remove PMMA using simple etching steps yields nanoporous films that can be used for high-resolution lithography, templated synthesis, or selective transport applications. We demonstrate successful spatial control of the deposition by manipulating the electric field at the substrate using a grid electrode. We find that the morphology in this system is principally dictated by the substrate temperature, with solvent composition and deposition rate playing a secondary role. Well-ordered and vertically aligned PMMA cylinders could be produced by high-temperature deposition on the substrate (at and above 150 °C), while mixed and disordered morphologies predominated at lower temperatures. Deposition on a neutral substrate resulted in vertically aligned and physically continuous PMMA domains, indicating effective homoepitaxy in the deposition process.

Experimental

PS-*b*-PMMA with a molecular weight of 73.5 kg/mol and PMMA weight fraction of 0.28 was purchased from Polymer Source. All solvents were used as received (Sigma Aldrich Corp.). ESD was conducted in the cone-jet mode as previously described.[15,16] Briefly, 0.03 wt% PS-*b*-PMMA solutions were fed into a stainless steel needle using a programmable syringe pump at flow rates of 3 μL/min for 20 min or 16 μL/min for 10 min. The needle (35 μm inner diameter and 110 μm outer diameter) was held at high voltage to act as a liquid atomizer. The resulting BCP films have thicknesses of 80–100 nm. The charged droplets generated under high voltage in the cone-jet mode were collected on piranha-treated silicon substrates or random copolymer neutralized substrates[15] placed on a temperature-controlled electrically grounded plate at prescribed temperatures between 105 and 195 °C at a distance of 3 cm from the needle tip. Patterned deposition was performed onto glass substrates at 3 μL/min and 195 °C using 0.03 wt% acetone solutions with high voltage applied to the copper grid, while the needle was kept grounded. The grid at high voltage was separated from the grounded heater plate by a thermally conductive and electrically insulating Kapton sheet and also slightly elevated by glass slides placed along its perimeter, leaving an air gap beneath the deposition area. The electric field in this configuration was simulated using ANSYS Maxwell software. Surface morphologies of sprayed films were characterized using Bruker Dimension Fastscan AFM under tapping mode. SEM imaging was carried out using Hitachi SU-70 at 2 kV accelerating voltage after samples were swollen using isopropanol and water mixture (volume ratio 6:4) at 70 °C to improve contrast between the PS and PMMA domains.

Results and discussion

The as-sprayed surface morphology of ESD films is a function of spray parameters such as the deposition temperature, flow rate of feed solution and solvent composition. Figure 1 demonstrates the effect of deposition temperature on electrosprayed PS-*b*-PMMA thin films sprayed from acetone solutions using low (3 μL/min) for 20 min and high flow rates (16 μL/min) for 10 min on a non-treated (preferential wetting for PMMA) substrate. With the increase of temperature from 105 to 195 °C, the film morphology evolved from one exhibiting globular structures indicative of non-relaxed polymer chains [Fig. 1(a)] to one displaying ordered PMMA microdomains with mixed orientations [Fig. 1(c)] to eventually a well-ordered film with near-perfect perpendicular morphology [Fig. 1(e)]. A similar trend

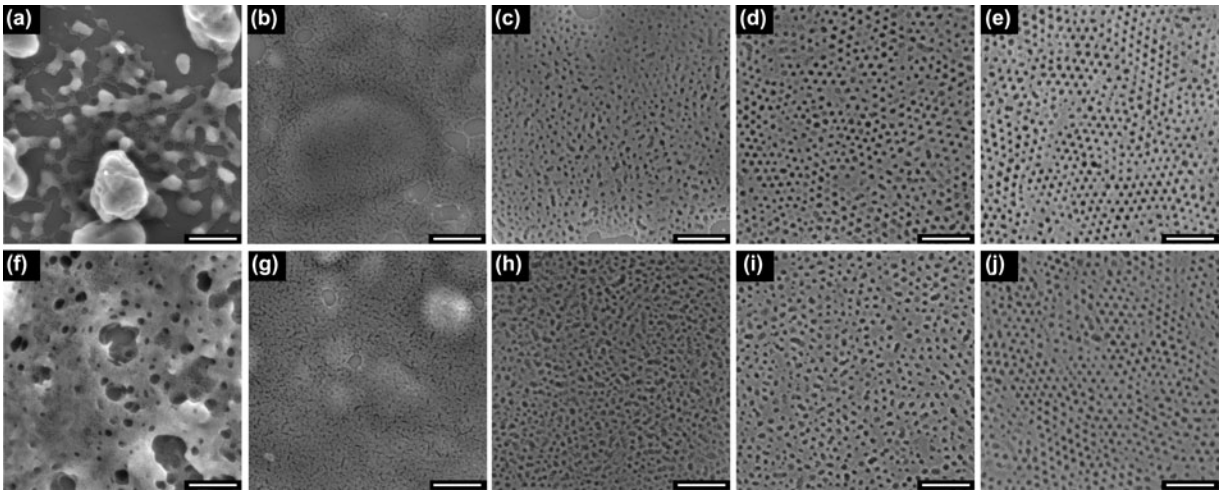


Figure 1. Effects of temperature and deposition rate on film morphology. Top-down SEM images of electrosprayed PS-*b*-PMMA thin films from acetone solution onto preferential substrates at low flow rate 3 μL/min (a–e) and high flow rate 16 μL/min (f–j) at substrate temperatures of 105 °C (a, f), 125 °C (b, g), 150 °C (c, h), 175 °C (d, i), and 195 °C (e, j). Scale bars: 200 nm.

https://doi.org/10.1557/mrc.2015.37 Published online by Cambridge University Press

was observed for films sprayed at the higher flow rate with little change in the microdomain orientation except at the lowest temperature of 105 °C. At this temperature a mostly smooth film with some circular features that resemble the PMMA cylinders was produced, Fig. 1(f).

The ordering kinetics in ESD is a combined result of solvent and thermal annealing.[16] PMMA preferentially wets the native silicone oxide surface of the silicon substrates due to its more polar nature relative to PS.[20] On the other hand, PS is expected to be present preferentially at the film–air interface due to its slightly lower surface energy[21] although this effect is temperature dependent.[20,22] The equilibrium morphology for the system is therefore one of PMMA cylinders orientated parallel to the substrate. Thus, the perpendicular orientation in Fig. 1 is not a result of substrate preference but more likely due to one or a combination of the following two reasons: a neutrality condition established at the solvent-mediated film–air interface as a function of temperature and/or kinetic trapping of morphology induced by the directional (vertical) solvent evaporation at deposition. The small difference in surface energy between PS and PMMA blocks (0.1 dyn/cm or <1%)[20,22] can be eliminated at high temperature, thereby creating a neutral film–air interface. Prior reports have shown that segregation of PS at the air interface can be suppressed by annealing at temperatures above 225 °C.[23] Perpendicular orientation nucleated from the neutral free interface can extend into films of 300–900 nm thickness when annealed at 230 °C on rough[24] or neutralized surfaces,[25] or when annealed at 170 °C with the addition of surfactants.[26] We observed similar effect in our study where the PMMA cylinders adopt perpendicular orientation at high deposition temperature of 175 to 195 °C. At the lower flow rate, solvent is expected to undergo near complete evaporation during droplet flight to the substrate[15] leaving little or no residual solvent for evaporation driven morphology. Instead, we speculate that the selectivity of acetone for PMMA versus PS might modify the wetting condition of the film–air interface to offset the small preference to PS thereby resulting in a less preferential interface favoring perpendicular orientation. This would account for the ability to achieve perpendicular oriented PMMA microdomains at lower temperatures in our study compared with the above discussed literature where no solvent effects are present. Reducing the deposition temperature would affect the system by decreasing the mobility of the polymer, changing the evaporation behavior of any residual solvent in arriving material and modifying the interfacial interactions of PS and PMMA. It is likely that the mobility effect is the most significant, accounting for the loss of order at 125 °C and non-relaxed films with micron-scale bumps imparted by globular structures produced on deposition at 105 °C.

The size of droplets generated in electrospray scales (d) with the flow rate (Q), $d \sim Q^{\alpha}$ with $\alpha = 1/3$ for high viscosity fluids with good conductivity and $\alpha = 1/2$ for low viscosity, poorly conducting fluids.[27] Larger droplets are produced at higher flow rates and require longer time for solvent evaporation.[27] Films sprayed at the higher flow rate here are therefore more susceptible to solvent effects due to a larger quantity of residual solvent present at deposition (droplet flight time is independent of droplet size, to a reasonable approximation). This is more so the case at lower deposition temperatures where convective heat transfer to the droplet is reduced in the vicinity of the substrate. It is apparent that the morphologies obtained from higher flow rates at high temperatures, Figs. 1(h)–1(j), display a subtle but discernable increase in defect density, as judged by the decrease in orientational and lateral order, compared with the ones sprayed at lower flow rates; Figs. 1(c)–1(e). The Fourier transforms of these images can be found in Supporting Information, Fig. S1. We suggest that this may be due to a larger than optimal or excessive rate of solvent removal. The solvent removal rate is a critical factor in determining the morphology of solvent vapor-annealed films. A gradual removal as measured by film deswelling is favored for eliminating defects as it permits sufficient time to organize into lower-energy configurations.[8] Similarly, the microdomain orientation in solvothermal annealing is sensitive to the rate of thermally induced solvent removal (deswelling) when both thermal annealing and solvent vapor are present, with fast quenching leading to less ordered films.[28] The rate of solvent removal in ESD (R_{evap}) can be estimated using a steady-state assumption and is expected to scale with the flow rate as $R_{evap} \sim Q^{1/2}$. In this scenario, the ~2.3× increase in the solvent removal rate brought by the higher flow rate acts to disrupt the morphology of the system. At the lowest temperature of 105 °C, films deposited at the high flow rate [Fig. 1(f)] is much smoother with some signs of nanoscale ordering, compared with that from the low flow rate [Fig. 1(a)]. This is consistent with the notion that there is a larger quantity of residual solvent available at the high flow rate deposition which assists in the wetting and relaxation of the film.

To further explore the effect of solvent, we examined films sprayed from different solvents as summarized in Fig. 2. Additional data sets for films sprayed from a wider variety of solvents [$CHCl_3$ and acetone, tetrahydrofuran (THF) and acetone, and THF and acetic acid] and relevant thermophysical solvent properties are available in Supporting Information Figs. S2–S4, Table S1. Note that acetone and acetic acid are added in small quantities (< 20 wt%) to improve the conductivity of the $CHCl_3$ and THF solutions to enable stable ESD in the cone-jet mode. The top row of Fig. 2 represents morphologies obtained at high temperature (195 °C) and the low flow rate (3 μL/min). Here, perpendicular orientations of the PMMA microdomains are observed with some, though not strong, variation in the lateral order for the different solvents. The bottom row of Fig. 2, on the other hand, demonstrates film morphology at low temperature (105 °C) and the high flow rate (16 μL/min). In this case, we observe a much stronger dependence of morphology on solvent composition, ranging from pockmarked films with poorly ordered but vertical PMMA domains, to mixed parallel and perpendicular PMMA microdomains, and even inversion of the morphology to discrete PS microdomains in a PMMA matrix.

It is apparent that the morphology produced in the high-temperature/low flow rate case is dominated by thermal

https://doi.org/10.1557/mrc.2015.37 Published online by Cambridge University Press

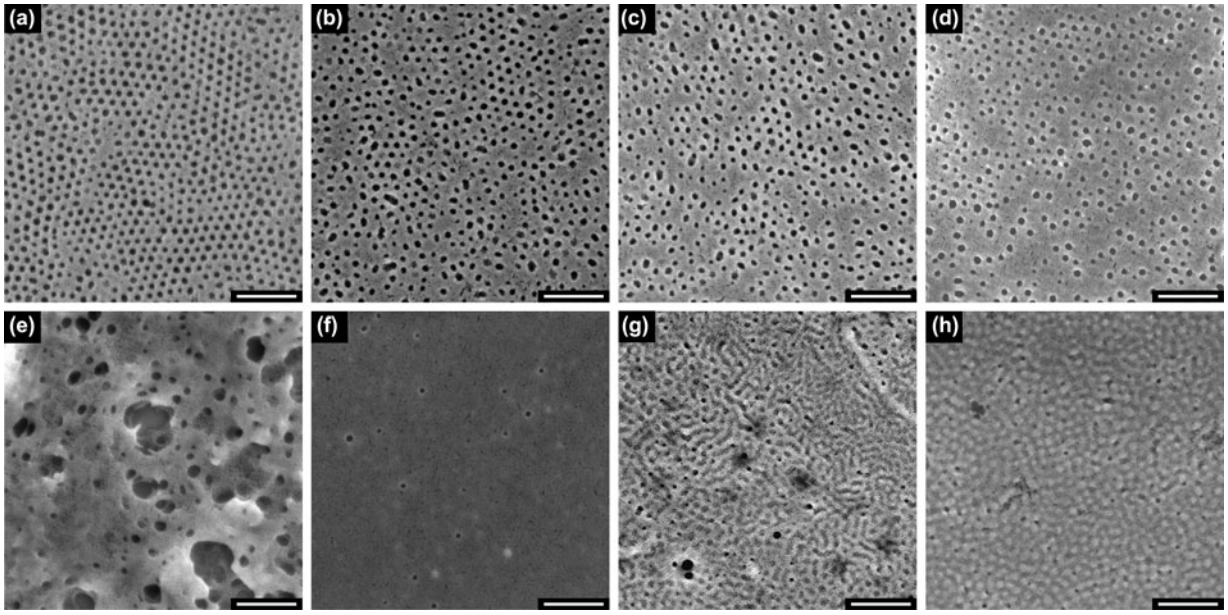


Figure 2. Effects of solvent composition under low flow/high-temperature conditions versus high flow/low-temperature deposition. Top-down SEM images of electrosprayed PS-*b*-PMMA thin film onto preferential substrates at low flow rate 3 μL/min, high temperature 195 °C (a–d) and high flow rate 16 μL/min, low temperature 105 °C (e–h) from solutions in acetone (a, e), $CHCl_3$ and acetone (volume ratio 8:2) (b, f), THF and acetone (volume ratio 8:2) (c, g), and THF and acetic acid (volume ratio 9:1) (d, h). Scale bars: 200 nm.

annealing, while that in the low-temperature/high flow regime is dominated by solvent effects. This is reasonable as there is less residual solvent at deposition in the low flow rate case. Conversely, the presence of substantially more residual solvent in the low-temperature/high flow rate situation and the resulting faster removal rate imply greater effects of solvent evaporation on the morphology. Additionally, the proximity of the deposition temperature to the nominal or melt-state value of the glass transition of the polymers makes their dynamics strongly sensitive to solvent interactions. The morphologies in this "solvent-dominant" regime signal a strong dependence on the selection of spray solvents. Reports in literature have discussed the sensitivity of PS-*b*-PMMA thin-film morphology to solvent annealing conditions, with morphologies ranging from disordered micellar structures, to highly ordered nanoscale spheres and stripes.[29–31] Compared with acetone, $CHCl_3$ is less selective is for PMMA, while THF is almost neutral for the system.[29,31] We observe a slight reduction of out-of-plane orientation of PMMA cylinders from Figs. 2(e) to 2(f), potentially due to less acetone in the solvent mixture to encourage that morphology. In fact, the morphology in these two cases is poorly developed, making it somewhat difficult to speak explicitly in terms of cylinder orientation. Since acetone is the most volatile and conductive solvent, droplets generated from acetone are expected to be the smallest and to evaporate the fastest, leaving the least amount of solvent at deposition to facilitate wetting and ordering of the film. Film smoothness, therefore, is improved when acetone is not the sole solvent. The PMMA cylinders start to adopt parallel orientations when deposited using a more neutral solvent, THF. Besides the change of solvent selectivity, THF is also the less volatile compared with acetone or $CHCl_3$. The combination of the presence of a more neutral solvent with a lower evaporation rate will favor parallel orientation in the solvent removal process.[32,33]

The morphology of films sprayed from THF and acetic acid [Fig. 2(h)] suggests phase inversion has occurred, PS cylinders or truncated lamellae appearing as lighter regions in the SEM images. Acetic acid is considered to be a good solvent for PMMA but it is non-solvent for PS, such that it is often used in selectively removing photodegraded PMMA from PS-*b*-PMMA films after UV exposure. The low volatility of acetic acid relative to THF means droplets become enriched in acetic acid due to differential evaporation during flight, relative to the starting concentration of the feed solution. This effect is amplified on deposition given the high boiling point of acetic acid (118 °C) relative to the deposition temperature (105 °C), which would therefore lead to preferential swelling of PMMA and collapse of the PS chains. It is clear that these effects are significant enough to invert the morphology of the system. The persistence of this highly non-equilibrium state is guaranteed by the fact that the system is kinetically trapped by the low substrate temperature relative to the nominal T_g, once all residual solvent has evaporated. The insolubility of PS in acetic acid is likely also the reason for the relatively poor ordering of films sprayed in the "thermal-dominant" region [Fig. 2(d)]. In this case, the arriving material, subject to an increase of volume fraction of non-solvent during flight, would require additional time or temperature to relax

https://doi.org/10.1557/mrc.2015.37 Published online by Cambridge University Press

into a well-ordered morphology relative to other cases [Figs. 2(a)–2(c)]. While the self-assembly during ESD in the "solvent-dominant" regime is in some sense more complicated than in the "thermal-dominant" regime, the strong variation of morphology provides a potentially useful handle for engineering structure in thin films. One can readily envision for example the potential to use vitrification of solvent-dictated morphologies produced at sub-T_g or near-T_g temperatures as a means to continuously grow vertically aligned domains by ESD. Work is continuing along this front.

On the other hand, the out-of-plane morphology realized here in the "thermal-dominant" region is unlikely to persist over longer deposition periods given the preferential nature of the substrate. We have previously reported the relaxation of poly(styrene-*block*-ethylene oxide) (PS-*b*-PEO) on preferential substrates and its reorganization into equilibrium parallel morphology over time, resulting in a morphology that varies as a function of depth in the film—newly deposited material shows vertical orientation while buried layers have relaxed into a parallel orientation.[15] Close examination of the films here reveals that the perpendicular orientation of PMMA cylinders in fact does not extend all the way to the bottom surface where a thin layer of PMMA is present in the vicinity of the substrate, Fig. S5. This is a result of the strong preferential wetting interaction at the substrate compared with the (temperature-dependent) neutral wetting from the free interface.[26] By utilizing a neutral substrate,[15] however, we were able to preserve the out-of-plane morphology and deposit well-ordered and vertically aligned PS-*b*-PMMA with arbitrary thickness ranging from 60 to 700 nm, Fig. 3. We note here that the microdomains are not only vertically aligned but also physically continuous. Such a situation becomes difficult and infeasible in thermally annealed films spin-coated onto neutral substrates as the perpendicular orientation has to propagate from the exterior surfaces.[25] By comparison, with ESD the orientation and physical continuity are realized in real time during deposition of the material. The physical continuity of the domains also makes it clear that the system exhibits homoepitaxy in that the PMMA domains are laterally registered throughout the depth of the film.

The use of electric field focusing to achieve patterned ESD is described in Fig. 4. In our setup, high-voltage bias (5 kV) was applied to the grid that was used to pattern the deposition, while the fluid feed needle was held at ground. For safety, the metallic heating stage was also grounded. While the potential of the glass substrate was not controlled, it is expected to be near ground. This setup inverts the typical arrangement in ESD in which the atomizing needle is charged relative to a grounded substrate. It was made necessary by the need to generate substantial lateral potential gradients at the substrate to drive the patterning—in the conventional arrangement the presence of a physically continuous grounded plate (the heating stage) in proximity to a grounded grid would significantly squash the gradients in potential due to the distant high-voltage source at the needle. The particular electric field patterns resulting from the arrangement are sensitive to the relative locations of the needle, substrate, grid and heating stage, as well as the permittivities of these and intervening layers (air, electrically insulating glass mounts, for example). The specification of the geometry and plots of the associated electric field are provided in Supporting Information Figs. S6 and S7, showing that majority of field lines pass between the atomizer and the gridlines of the copper mesh.

The results of deposition in this configuration are shown in Figs. 4(c) and 4(f). The pattern of the electrode grid is reproduced by the polymer but it is apparent that there is a loss of fidelity in the reproduction. We quantify this simply by the ratio of the linewidth of the electrode feature in the polymer relative to the feature size in the electrode mask, $\varphi = t_p/t_m$. Across

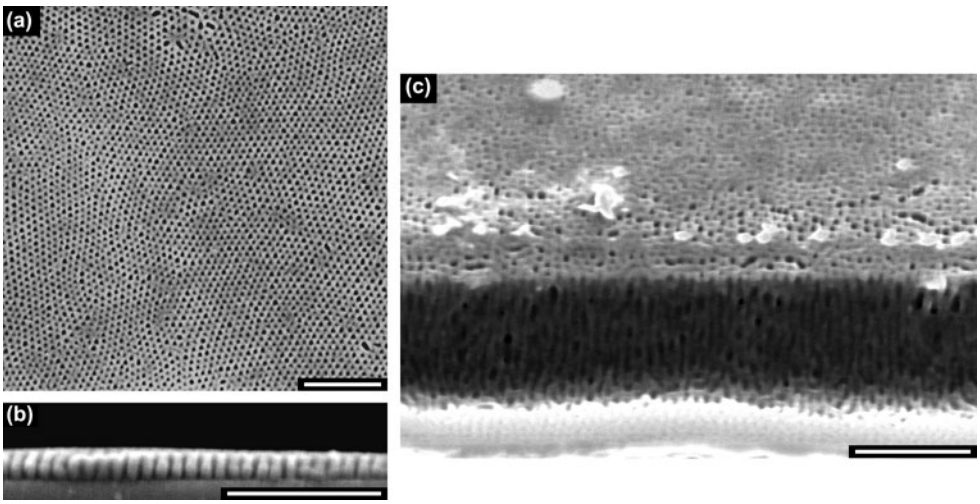


Figure 3. SEM images of well-ordered and vertically aligned (a, b) 60 nm and (c) 700 nm thick PS-*b*-PMMA on neutralized substrate. (a) Top-down view; (b) cross-sectional view; and (c) tilted view, with bottom of film slightly curled upwards. Scale bars: 400 nm.

https://doi.org/10.1557/mrc.2015.37 Published online by Cambridge University Press

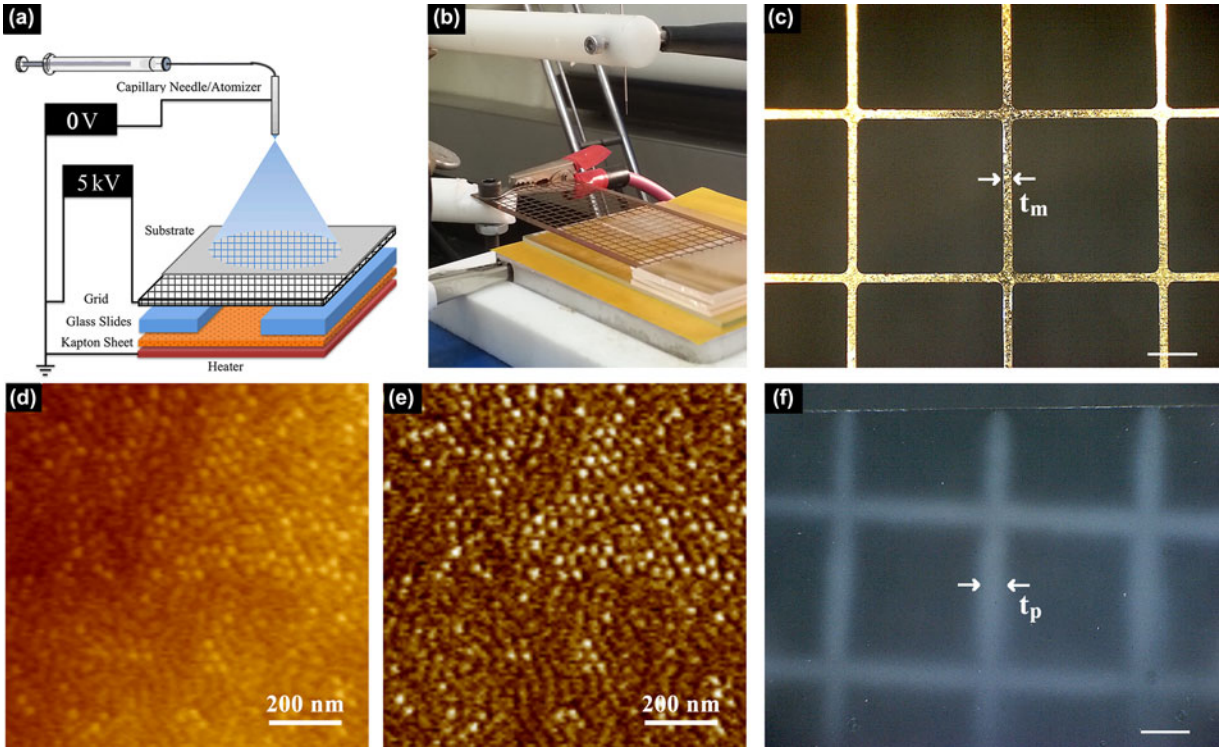


Figure 4. "Positive" pattern deposition of PS-*b*-PMMA using patterned electrode (copper grid) to guide the polymer deposition carried in charged droplet along the electrical field line. (a) Schematic representations of the process, (b) experimental setup, optical image of (c) the mesh, and (f) the deposited glass substrate, scale bar represents 1 mm, (d) height and (e) phase image of patterned/opaque region of the substrate in (f) deposited at substrate temperature of ~150 °C.

the deposited area, on average, φ ranges from 2 to 3. There is some spatial dependence that appears to derive simply from inconsistency in the spacing between the electrode grid and the deposition substrate due both to electrostatic attraction to the grounded heater which acts to bend the grid (the electrode is free standing in the space between the glass supports) and simple misalignment and imperfection of the brass grid. The patterned regions of PS-*b*-PMMA display an ordered morphology, Figs. 4(d) and 4(e), with mixed orientations of the PMMA microdomains. While the heater was held at 180 °C, the separation of the substrate from the heater and the poor thermal conductivity of the intervening layers implies that the substrate temperature would be considerably lower. We estimate the temperature to be 155–160 °C, using reference values for the thermal conductivity of ambient air, Kapton, borosilicate glass, and the brass of the grid electrode. This may explain the decrease in the level of order compared with the non-patterned films. Additionally, the reduced deposition area provided by the electrode pattern resulted in a ~10-fold increase of the deposition rate of the BCP. This is likely the reason for the cloudiness of the films, which mimics the cloudiness of non-patterned films deposited at similarly high rates.

We expect that we can improve the morphological control of our process, for example by simply calibrating the setup to better control temperature and deposition distance. Similarly, the fidelity can also be significantly improved through better optimization of the relative separations of the substrate, grid and heater from the needle. The simulations clearly show that the potential difference between the grid and the center of the opening between grids is about 800 V, which leads to an enhancement to drive deposition of only 20% in the electric field in the patterned regions (Supporting Information, Fig. S8). There are additional opportunities to concentrate the electric fields through the use of floating electrodes. These are being pursued using guidance from finite element simulations. Finally, an alternative way of patterning deposition is to utilize an electrode grid/mask above, rather than below, the collecting substrate. Apart from the physical masking effect, one can engineer electrostatic focusing due to the bias between the mask and the substrate such that the spot size produced is substantially smaller than the opening between the grid lines.

Conclusion

In summary, we have demonstrated the use of electrospray for continuous deposition, and continuous patterned deposition of ordered PS-*b*-PMMA thin films on preferential and neutral substrates. Thin-film morphology on preferential substrates is dependent on solvent selection, deposition temperature, and flow rate of the feed solution, which can be tuned to manipulate thermal and/or solvent annealing in the process. In the

https://doi.org/10.1557/mrc.2015.37 Published online by Cambridge University Press

"thermal-dominant" regime where a high deposition temperature and a low flow rate are used, perpendicular orientation of PMMA cylinders is favored due to the neutralization of the film–air interface at high temperature further assisted by PMMA-selective solvent. Conversely, in the "solvent-dominant" regime the film morphology is much more sensitive to the solvent selection, with solvent selectivity and solvent removal rate collectively determining the morphology of the film. Vertically aligned and physically continuous microdomains can be produced on neutralized substrates over a wide thickness range. Electrical fields are controlled using patterned electrode to direct the location of charged droplets, which eventually yields patterned deposition of BCP thin films. Thin film patterns of PS-*b*-PMMA largely replicate the original shape of the metal grid with ordered morphology, although there is need and room for significant improvement. The ability to conduct near-dry electrospray enables sequential deposition of without disruption of underlying layers. We can therefore contemplate the use of ESD to assemble compositionally and structurally heterogeneous thin films with spatial control enacted through a switchable electrode array, for example. Taken together, the results here may provide new opportunities for engineering functional BCP thin films.

Supplementary materials

For supplementary material for this article, please visit http://dx.doi.org/10.1557/mrc.2015.37

Acknowledgments

The authors gratefully acknowledge support from NSF DMR-1410568 and additional funding from CMMI-1246804. C.O. acknowledges additional financial support from ONR YIP award N000141210657 and a 3M Nontenured Faculty Award. Facilities use was supported by YINQE and NSF MRSEC DMR-1119826. The authors thank Dr. Jonathan Singer for helpful discussions during the execution of this work. PG and MYK acknowledge partial support from NSF through a grant to the Nanoscale Science and Engineering Center at UW-Madison (DMR-0832760).

References

1. H.Q. Hu, M. Gopinadhan, and C.O. Osuji: Directed self-assembly of block copolymers: a tutorial review of strategies for enabling nanotechnology with soft matter. *Soft Matter* **10**, 3867 (2014).
2. E. Han, K.O. Stuen, Y.H. La, P.F. Nealey, and P. Gopalan: Effect of composition of substrate-modifying random copolymers on the orientation of symmetric and asymmetric diblock copolymer domains. *Macromolecules* **41**, 9090 (2008).
3. D.Y. Ryu, K. Shin, E. Drockenmuller, C.J. Hawker, and T.P. Russell: A generalized approach to the modification of solid surfaces. *Science* **308**, 236 (2005).
4. J. Bang, J. Bae, P. Lowenhielm, C. Spiessberger, S.A. Given-Beck, T.P. Russell, and C.J. Hawker: Facile routes to patterned surface neutralization layers for block copolymer lithography. *Adv. Mater.* **19**, 4552 (2007).
5. R.D. Peters, X.M. Yang, T.K. Kim, and P.F. Nealey: Wetting behavior of block copolymers on self assembled films of alkylchlorosiloxanes: effect of grafting density. *Langmuir* **16**, 9620 (2000).
6. R.D. Peters, X.M. Yang, T.K. Kim, B.H. Sohn, and P.F. Nealey: Using self-assembled monolayers exposed to X-rays to control the wetting behavior of thin films of diblock copolymers. *Langmuir* **16**, 4625 (2000).
7. K.W. Gotrik, A.F. Hannon, J.G. Son, B. Keller, A. Alexander-Katz, and C.A. Ross: Morphology control in block copolymer films using mixed solvent vapors. *ACS Nano* **6**, 8052 (2012).
8. J.N.L. Albert, W.S. Young, R.L. Lewis, T.D. Bogart, J.R. Smith, and T.H. Epps: Systematic study on the effect of solvent removal rate on the morphology of solvent vapor annealed ABA triblock copolymer thin films. *ACS Nano* **6**, 459 (2012).
9. X.D. Gu, I. Gunkel, A. Hexemer, W.Y. Gu, and T.P. Russell: An in situ grazing incidence X-ray scatterings study of block copolymer thin films during solvent vapor annealing. *Adv. Mater.* **26**, 273 (2014).
10. G. Singh, S. Batra, R. Zhang, H.Y. Yuan, K.G. Yager, M. Cakmak, B. Berry, and A. Karim: Large-scale roll-to-roll fabrication of vertically oriented block copolymer thin films. *ACS Nano* **7**, 5291 (2013).
11. Z. Qiang, Y.Z. Zhang, J.A. Groff, K.A. Cavicchi, and B.D. Vogt: A generalized method for alignment of block copolymer films: solvent vapor annealing with soft shear. *Soft Matter* **10**, 6068 (2014).
12. S. Pujari, M.A. Keaton, P.M. Chaikin, and R.A. Register: Alignment of perpendicular lamellae in block copolymer thin films by shearing. *Soft Matter* **8**, 5358 (2012).
13. M.S. Onses, C. Song, L. Williamson, E. Sutanto, P.M. Ferreira, A.G. Alleyne, P.F. Nealey, H. Ahn, and J.A. Rogers: Hierarchical patterns of three-dimensional block-copolymer films formed by electrohydrodynamic jet printing and self-assembly. *Nat. Nanotechnol.* **8**, 667 (2013).
14. C.B. Tang, W. Wu, D.M. Smilgies, K. Matyjaszewski, and T. Kowalewski: Robust control of microdomain orientation in thin films of block copolymers by zone casting. *J. Am. Chem. Soc.* **133**, 11802 (2011).
15. H.Q. Hu, S. Rangou, M. Kim, P. Gopalan, V. Filiz, A. Avgeropoulos, and C.O. Osuji: Continuous equilibrated growth of ordered block copolymer thin films by electrospray deposition. *ACS Nano* **7**, 2960 (2013).
16. H.Q. Hu, J.P. Singer, and C.O. Osuji: Morphology development in thin films of a lamellar block copolymer deposited by electrospray. *Macromolecules* **47**, 5703 (2014).
17. J.W. Kim, Y. Yamagata, B.J. Kim, and T. Higuchi: Direct and dry micropatterning of nano-particles by electrospray deposition through a microstencil mask. *J. Micromech. Microeng.* **19**, 025021 (2009).
18. J.W. Xie, A. Rezvanpour, C.H. Wang, and J.S. Hua: Electric field controlled electrospray deposition for precise particle pattern and cell pattern formation. *AICHE J.* **56**, 2607 (2010).
19. X. Zhang and Y. Zhao: Programmable patterning of polymeric microparticles by floating electrodes-assisted electrospray. *J. Micromech. Microeng.* **22**, 047001 (2012).
20. T.P. Russell, G. Coulon, V.R. Deline, and D.C. Miller: Characteristics of the surface-induced orientation for symmetric diblock Ps/Pmma copolymers. *Macromolecules* **22**, 4600 (1989).
21. P.F. Green, T.M. Christensen, T.P. Russell, and R. Jerome: Equilibrium surface-composition of diblock copolymers. *J. Chem. Phys.* **92**, 1478 (1990).
22. P. Mansky, Y. Liu, E. Huang, T.P. Russell, and C.J. Hawker: Controlling polymer-surface interactions with random copolymer brushes. *Science* **275**, 1458 (1997).
23. P. Mansky, T.P. Russell, C.J. Hawker, J. Mays, D.C. Cook, and S.K. Satija: Interfacial segregation in disordered block copolymers: effect of tunable surface potentials. *Phys. Rev. Lett.* **79**, 237 (1997).
24. E. Sivaniah, Y. Hayashi, S. Matsubara, S. Kiyono, T. Hashimoto, K. Kukunaga, E.J. Kramer, and T. Mates: Symmetric diblock copolymer thin films on rough substrates. Kinetics and structure formation in pure block copolymer thin films. *Macromolecules* **38**, 1837 (2005).
25. E. Han, K.O. Stuen, M. Leolukman, C.C. Liu, P.F. Nealey, and P. Gopalan: Perpendicular orientation of domains in cylinder-forming block copolymer thick films by controlled interfacial interactions. *Macromolecules* **42**, 4896 (2009).
26. J.G. Son, X. Bulliard, H.M. Kang, P.F. Nealey, and K. Char: Surfactant-assisted orientation of thin diblock copolymer films. *Adv. Mater.* **20**, 3643 (2008).
27. A.M. Ganan-Calvo, J. Davila, and A. Barrero: Current and droplet size in the electrospraying of liquids. Scaling laws. *J. Aerosol Sci.* **28**, 249 (1997).

https://doi.org/10.1557/mrc.2015.37 Published online by Cambridge University Press

28. K.W. Gotrik and C.A. Ross: Solvothermal annealing of block copolymer thin films. *Nano Lett.* **13**, 5117 (2013).
29. J. Peng, D.H. Kim, W. Knoll, Y. Xuan, B.Y. Li, and Y.C. Han: Morphologies in solvent-annealed thin films of symmetric diblock copolymer. *J. Chem. Phys.* **125**, 064702 (2006).
30. Y. Chen, H.Y. Huang, Z.J. Hu, and T.B. He: Lateral nanopatterns in thin diblock copolymer films induced by selective solvents. *Langmuir* **20**, 3805 (2004).
31. Y. Xuan, J. Peng, L. Cui, H.F. Wang, B.Y. Li, and Y.C. Han: Morphology development of ultrathin symmetric diblock copolymer film via solvent vapor treatment. *Macromolecules* **37**, 7301 (2004).
32. W.A. Phillip, M.A. Hillmyer, and E.L. Cussler: Cylinder orientation mechanism in block copolymer thin films upon solvent evaporation. *Macromolecules* **43**, 7763 (2010).
33. G. Kim and M. Libera: Morphological development in solvent-cast polystyrene-polybutadiene-polystyrene (SBS) triblock copolymer thin films. *Macromolecules* **31**, 2569 (1998).

https://doi.org/10.1557/mrc.2015.37 Published online by Cambridge University Press